Selective detection of sulfide in human lung cancer cells with blue-fluorescence "ON-OFF-ON" benzimidazole-based chemosensor ensemble

Chak-Shing Kwan,† Tao Wang,† Sing-Ming Chan,† Zongwei Cai,* and Ken Cham-Fai Leung*

Department of Chemistry and State Key Laboratory of Environmental and Biological Analysis, The Hong Kong Baptist University, Kowloon Tong, Kowloon, Hong Kong SAR, P. R. China.

*E-mail: zwcai@hkbu.edu.hk
Tel: (+852) 3411 7070

*E-mail: cfleung@hkbu.edu.hk
Tel: (+852) 3411 2319
Fax: (+852) 3411 7348

Supplementary Information

Experimental Section

General Methods

Thin-layer chromatography (TLC) was performed on aluminum plate, and the plates were visualized by UV light, staining with phosphomolybdic acid or ninhydrin with heating. Column chromatography purification was performed on silica gel (SiO_2) 60F (Merck 9385, 0.040–0.063 mm). ^1H NMR and ^{13}C NMR spectra characterization were recorded at 298K with a spectrometer Bruker Avance-III (^1H: 400 MHz and ^{13}C: 101 MHz). Chemical shifts of solvent ($CDCl_3$, CD_3CN) were calibrated reference to the proton solvent residue peak ($CDCl_3$ = 7.26 ppm, d_6-DMSO = 2.50 ppm, CD_3CN = 1.94 ppm, D_2O = 4.79 ppm) and carbon solvent residue peak ($CDCl_3$ = 77.16 ppm, d_6-DMSO = 39.52 ppm, CD_3CN = 1.32 ppm). Coupling constants (J) were reported in hertz (Hz), with standard abbreviations indicating the multiplicity of the peaks (s = singlet, d = doublet, t = triplet, q = quartet, quin = quintet, m = multiplet, br = broad).

UV-Vis Absorption Spectrum

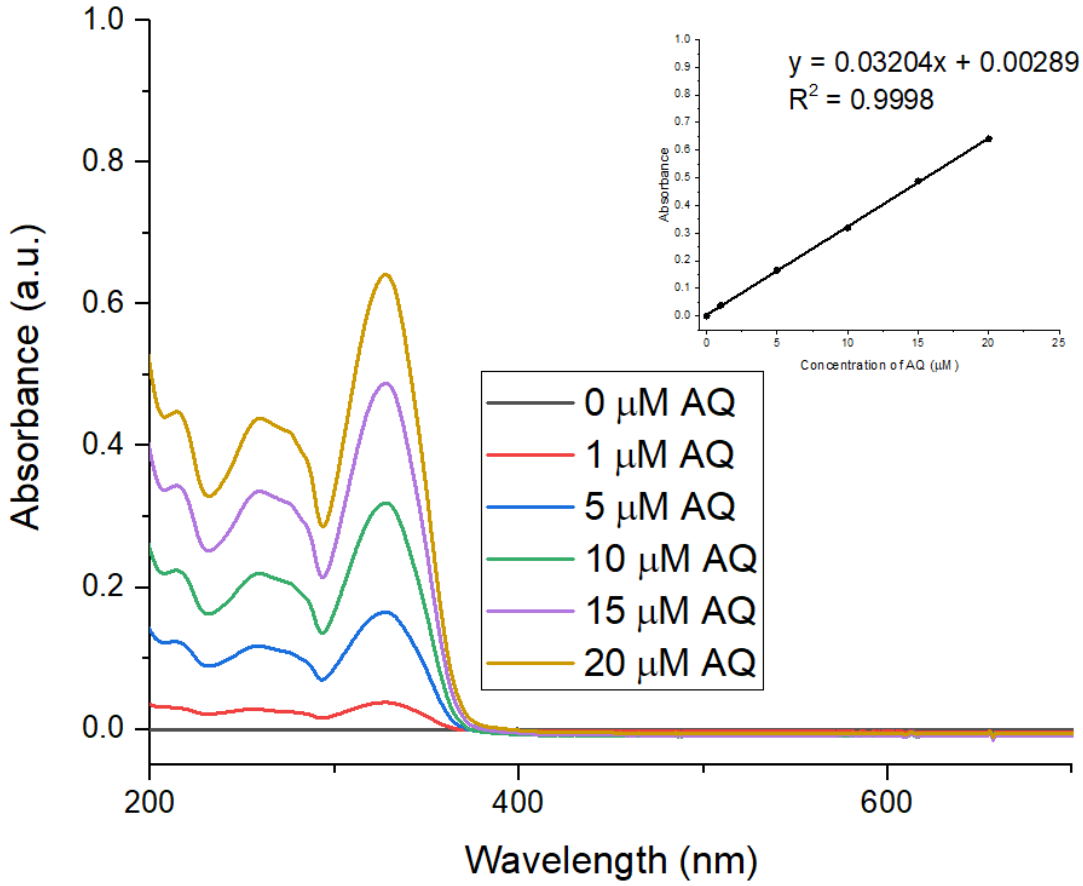

Figure S1. Absorption spectra of **AQ** (0.0 - 20.0 μM) in water (B), inserted graph is the Absorption of **AQ** (0.0 - 20.0 μM) at 328 nm.

Quantum yield measurement

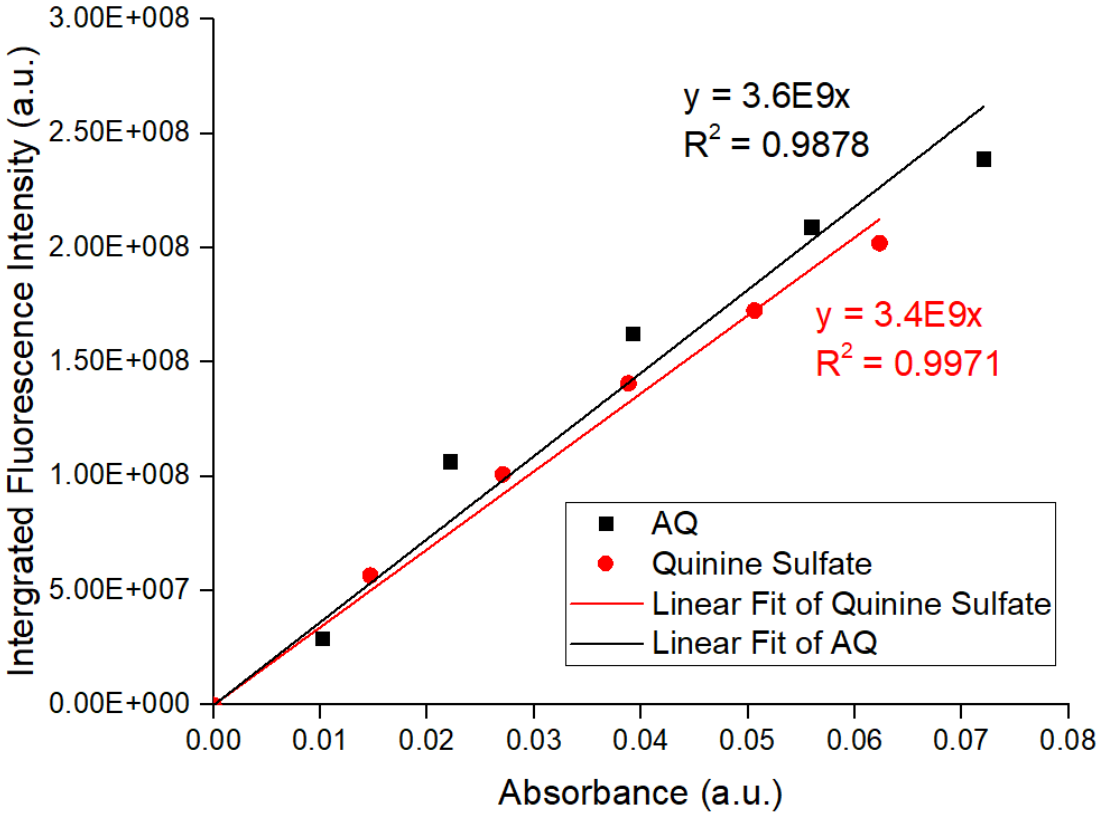

Figure S2. Integrated Fluorescence Intensity against absorbance of **AQ** and quinine sulfate.

The quantum yield of **AQ** were measured by comparative method with Quinine sulfate as the standard. Quinine sulfate in 0.1 M H_2SO_4 was prepared and used in the measurement with the excitation wavelength of 340 nm.

The integrated fluorescent intensity of the **AQ** and quinine sulfate was determined by integrating the whole as-obtained fluorescent spectrum using an Origin program. The integrated fluorescent intensity of the standard and the samples were plotted against the absorbances. Linear regression was performed on the plot and, and the slope of the plots were obtained. Quantum yield was calculated by the following equation:

$$\Phi = \Phi_{ref}\left(\frac{I}{A}\right)\left(\frac{A_{ref}}{I_{ref}}\right)\left(\frac{\eta^2}{\eta^2{}_{ref}}\right)$$

I is the integrated fluorescence intensity and A is the absorbance at the excitation wavelength. η is the refractive index of the solution and Φ is the quantum yield. Both 0.1 M H_2SO_4 and water have a refractive index of 1.33. The absorbances of analyte are kept below A = 0.1 in order to avoid interference.

The results in graph of integrated fluorescence intensity *vs* absorbance was used to determined I/A.

$I/A = 3.63 \times 10^9$

$I_{ref}/A_{ref} = 3.41 \times 10^9$

$\Phi_{ref} = 0.54$, $\Phi = 0.575$.

Fluorescence Spectra

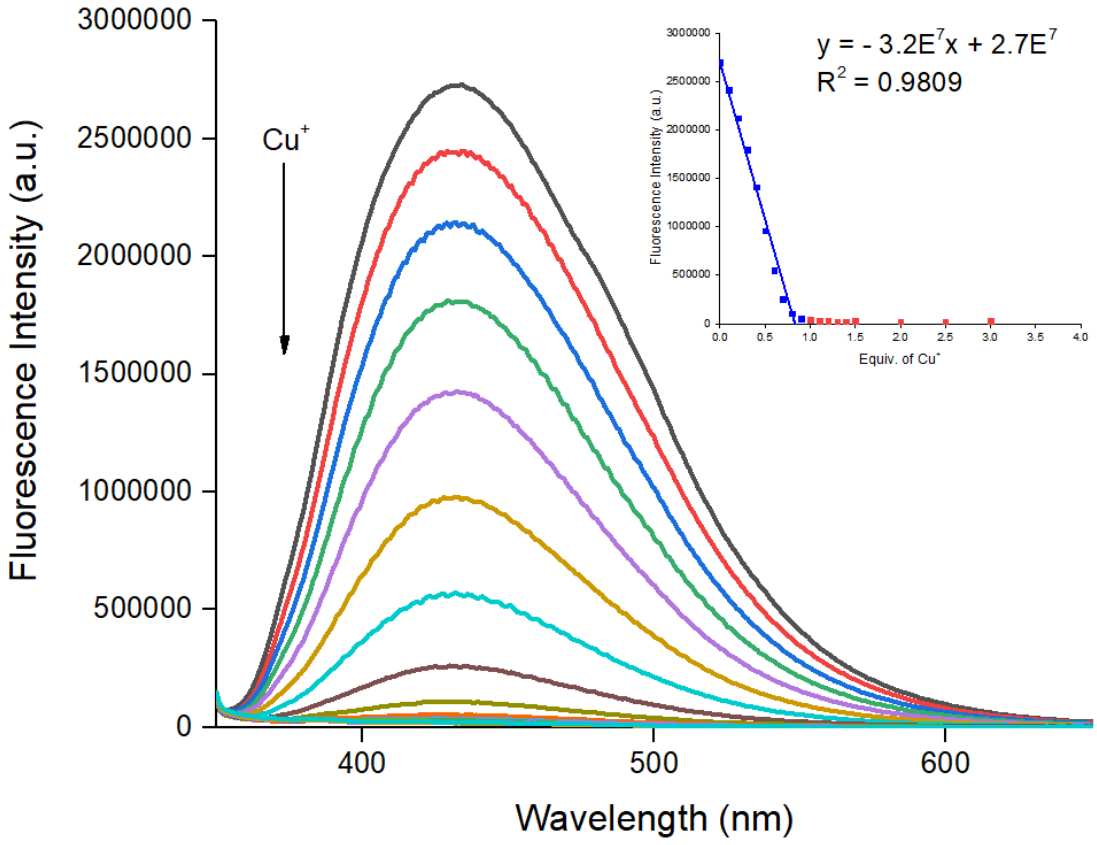

Figure S3. Fluorescence spectra of **AQ** (5 μM of **AQ**, λ_{ex} = 340 nm, 2% MeCN in H_2O, slit width: 1.5 nm/1.5 nm) upon the addition of Cu^+ (B), inserted graph is the fluorescence signal of **AQ** at 425 nm, upon the addition of Cu^+.

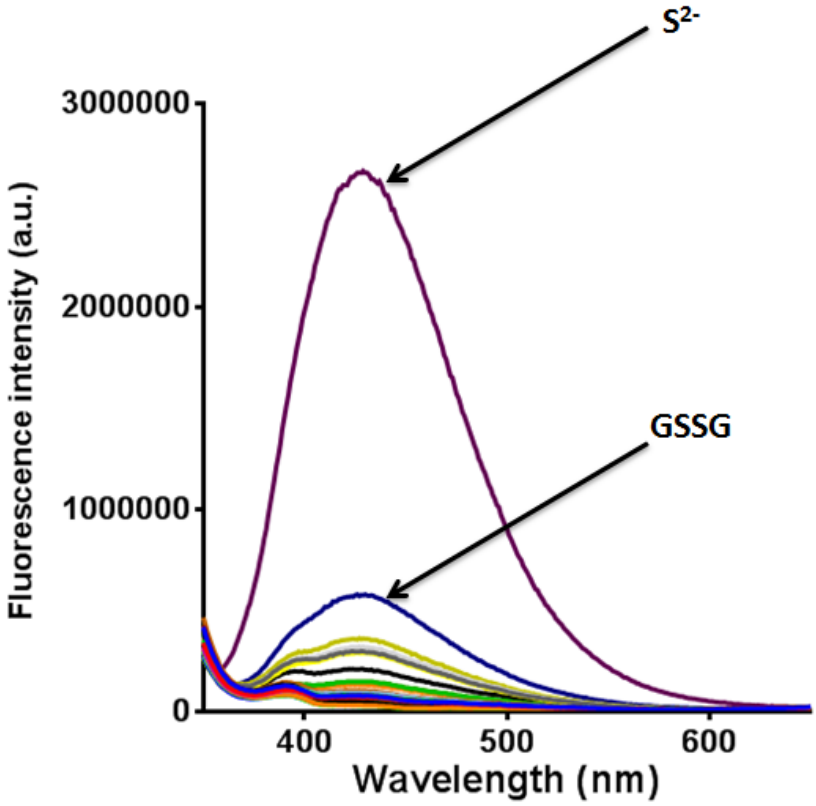

Figure S4. Fluorescence spectra of pre-formed **AQ**-Cu^{2+} (5 μM of **AQ** and 10 μM Cu^{2+}, λ_{ex} = 340 nm, pure H_2O, slit width: 1.5 nm/1.5 nm) upon the addition of 20 equiv. of anions.

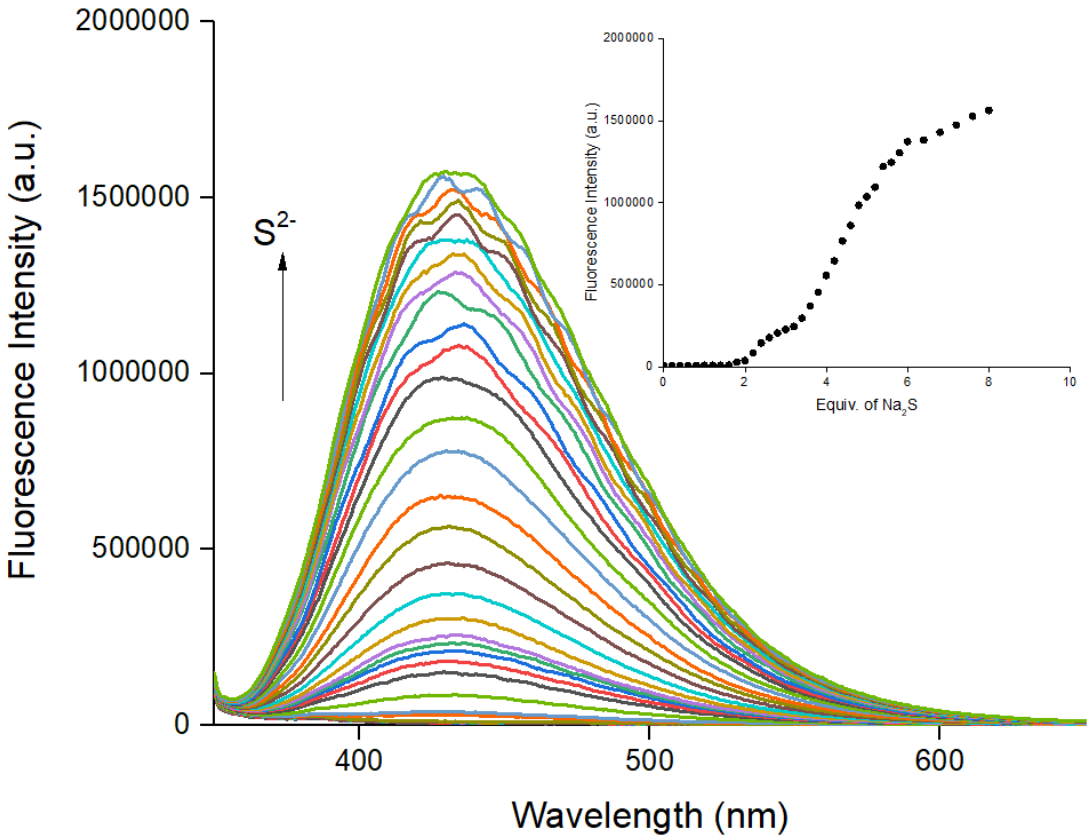

Figure S5. Fluorescence spectra of **AQ-Cu**$^{+}$ (5 μM of **AQ**, 10 μM of Cu^{+}, λ_{ex} = 340 nm, 0.5% MeCN in H_2O, slit width: 1.5 nm/1.5 nm) upon the addition of Na_2S (B), inserted graph is the fluorescence signal of **AQ-Cu**$^{+}$ at 425 nm, upon the addition of Na_2S.

Binding Constant Calculation

The calculation of binding constants (K_a) of **AQ** was determined by the Benesi–Hildebrand equation: $K_a = 1/(m(I_{max} - I_o))$.[S1] Where m is the slope of the graph $1/(I - I_o)$ against $1/[Cu^{2+}]$.

I_o = 1824280 ($[Cu^{2+}]$ = 0.0μM, 0.0 equiv.)

I_{max} = 57127 ($[Cu^{2+}]$ = 4.0 μM, 0.8 equiv.)

Table S1. Variable number used in Benesi–Hildebrand equation.

Equiv	$1/[Cu^{2+}]$	$I - I_o$	$1/(I - I_o)$
0.00	/	0	/
0.10	2000000.00	-368180.00	-2.72E-06
0.20	1000000.00	-594740.00	-1.68E-06
0.30	666666.67	-814230.00	-1.23E-06
0.40	500000.00	-1019404.00	-9.81E-07
0.50	400000.00	-1261117.00	-7.93E-07
0.60	333333.33	-1473748.00	-6.79E-07
0.70	285714.29	-1666362.00	-6.00E-07
0.80	250000.00	-1767152.90	-5.66E-07

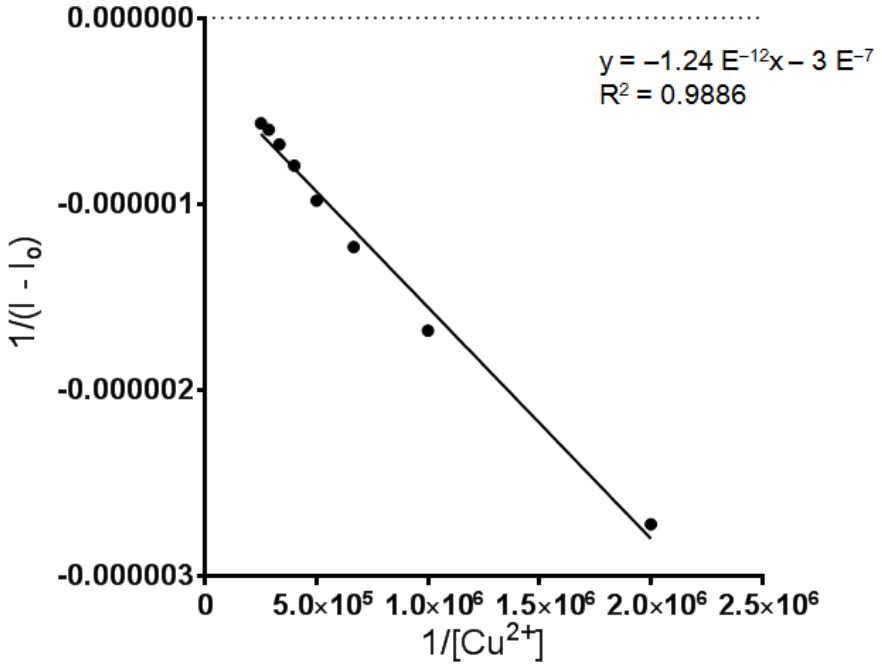

Figure S6. Benesi–Hildebrand Plot of **AQ** (5 μM) upon addition of Cu^{2+} and slope = -1.24×10^{-12}.

Hildebrand equation: $K_a = 1/(m(I_{max} - I_o))$

$K_a = 1/(-1.24 \times 10^{-12}(57127 - 1824280))$

$K_a = 4.56 \times 10^5\ M^{-1}$

Responsive Time Study

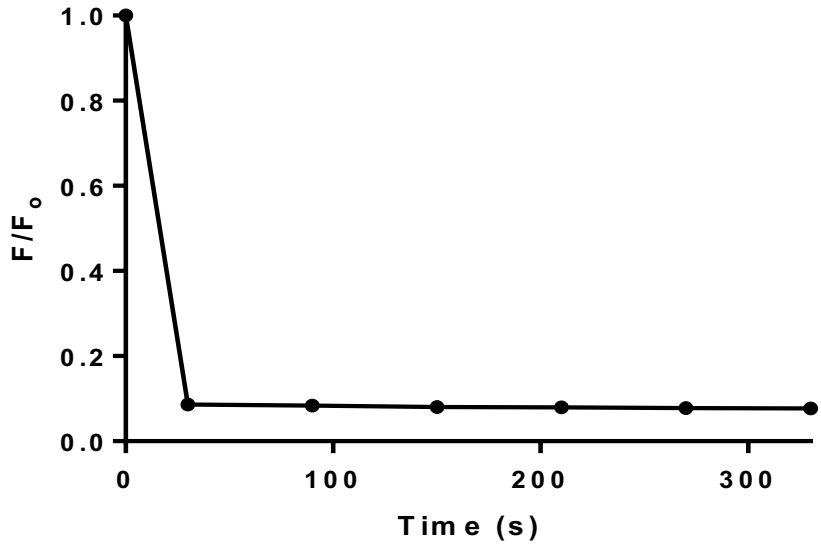

Figure S7. Fluorescence responsive time scanning at 425 nm of **AQ** (5 μM, λ_{ex} = 340 nm, pure H_2O, slit width: 1.5 nm/1.5 nm) after the addition of 10 equiv. of Cu^{2+}.

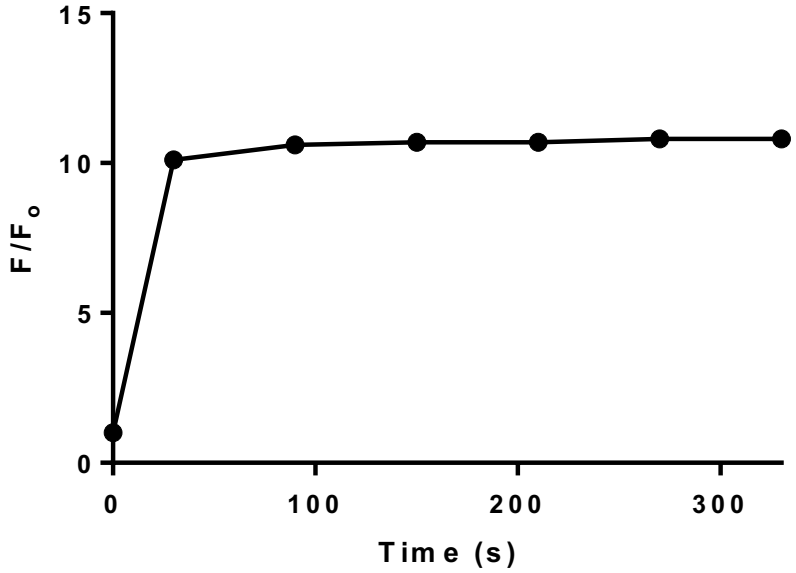

Figure S8. Fluorescence responsive time scanning at 425 nm of pre-formed **AQ**-Cu^{2+} (5 μM, λ_{ex} = 340 nm, pure H_2O, slit width: 1.5 nm/1.5 nm) after the addition of 10 equiv. of S^{2-}.

Ag^+ and Hg^{2+} study

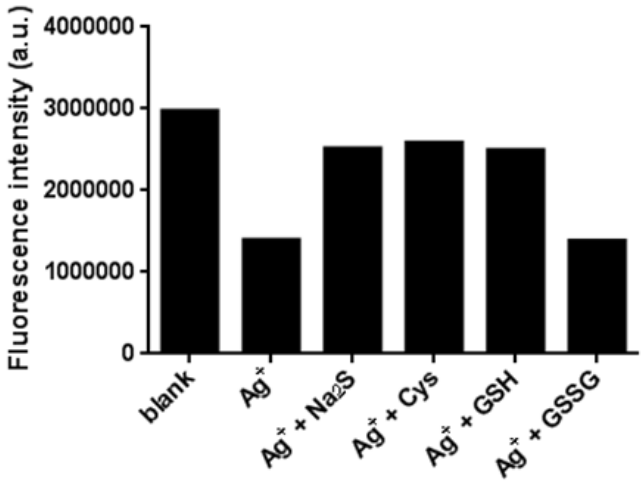

Figure S9. Fluorescence respond at 425 nm (5 μM, λ_{ex} = 340 nm, pure H_2O, slit width: 1.5 nm/1.5 nm) of **AQ**-Ag^+ toward different biothiols.

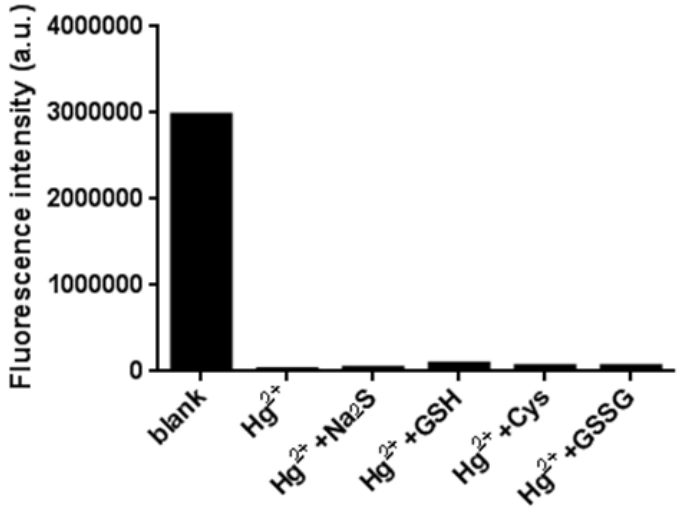

Figure S10. Fluorescence respond at 425 nm (5 μM, λ_{ex} = 340 nm, pure H_2O, slit width: 1.5 nm/1.5 nm) of **AQ**-Hg^{2+} toward different biothiols.

AQ-Cu^{+} and Aq-Cu^{2+} fluorescence study towards S^{2-}

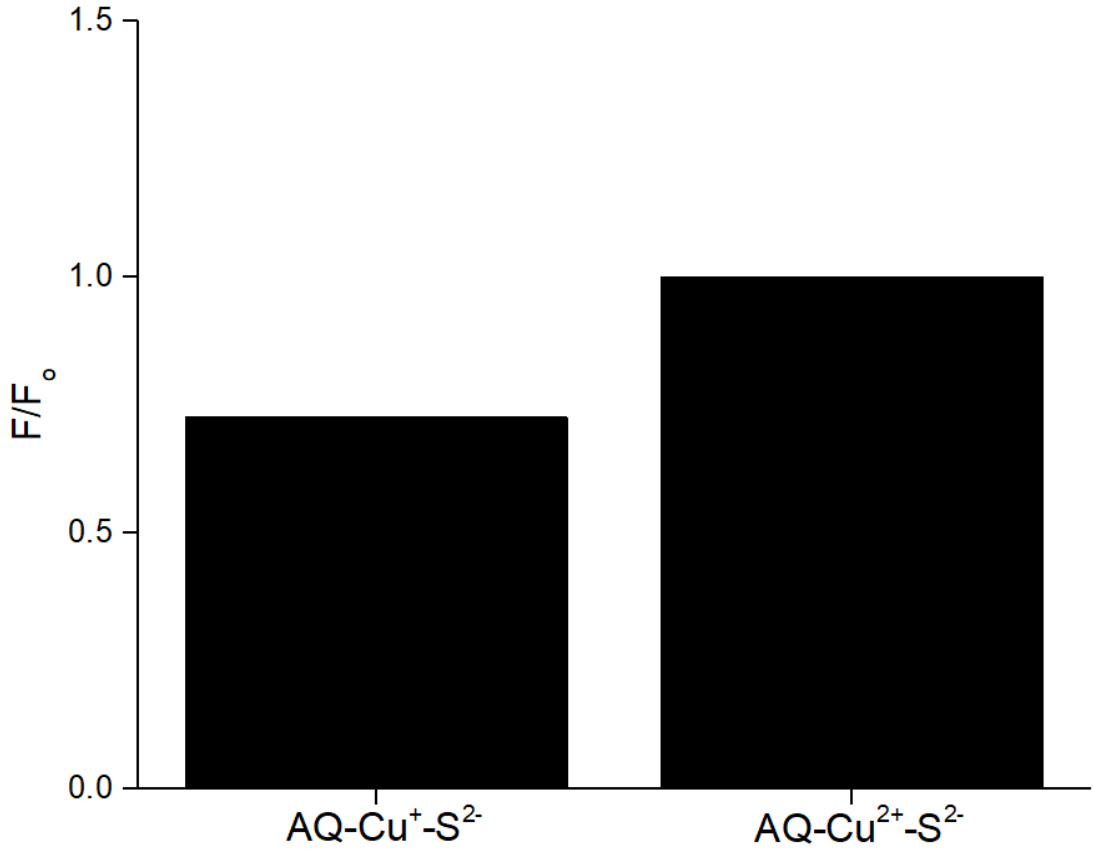

Figure S11. Fluorescence respond at 425 nm (5 μM, λ_{ex} = 340 nm, pure H_2O, slit width: 1.5 nm/1.5 nm) of **AQ**-Cu^{+} and **AQ**-Cu^{2+} toward S^{2-}.

NMR Titration

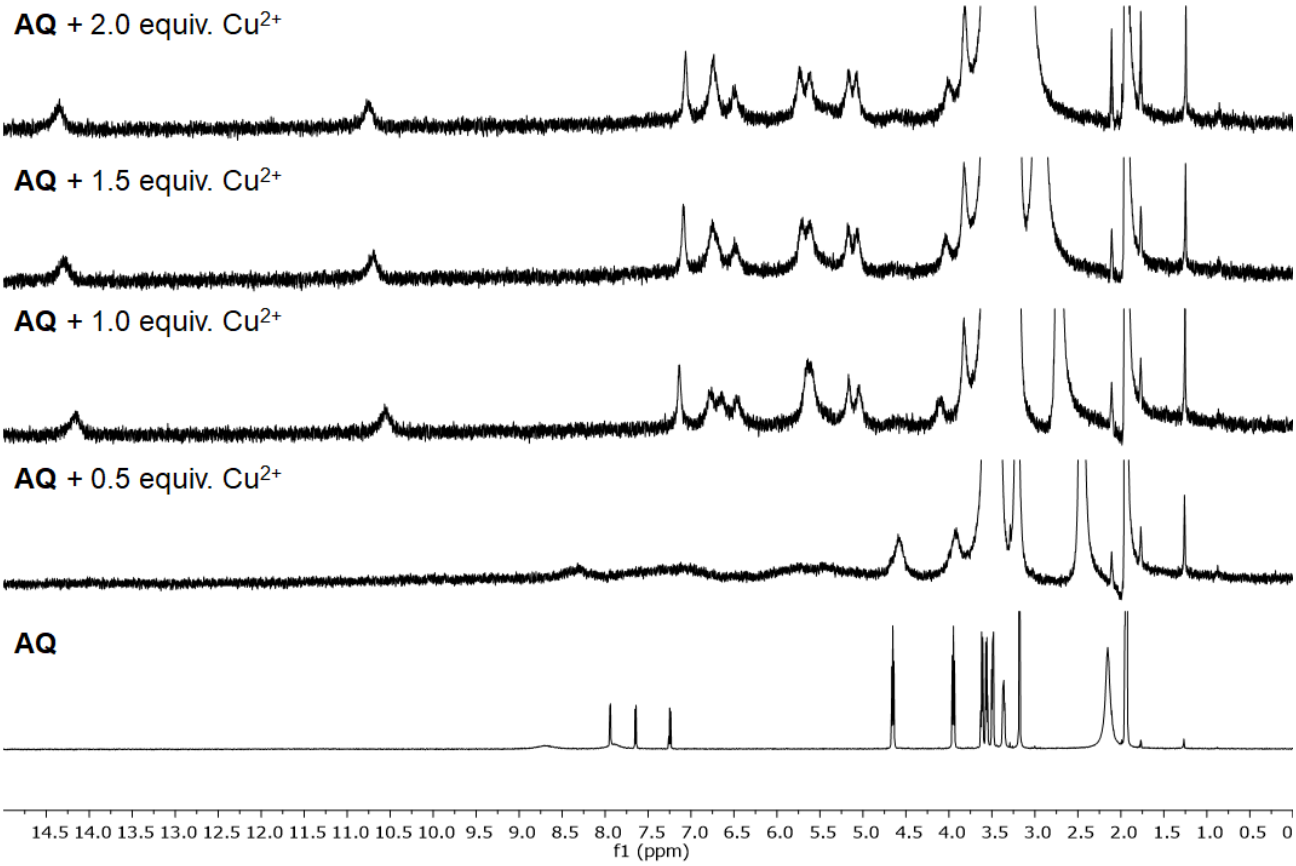

Figure S12. Stacked ^{1}H NMR spectra (400 MHz, CD3CN, 298 K) of **AQ** (5 mM) upon titration with different amount of Cu^{2+}.

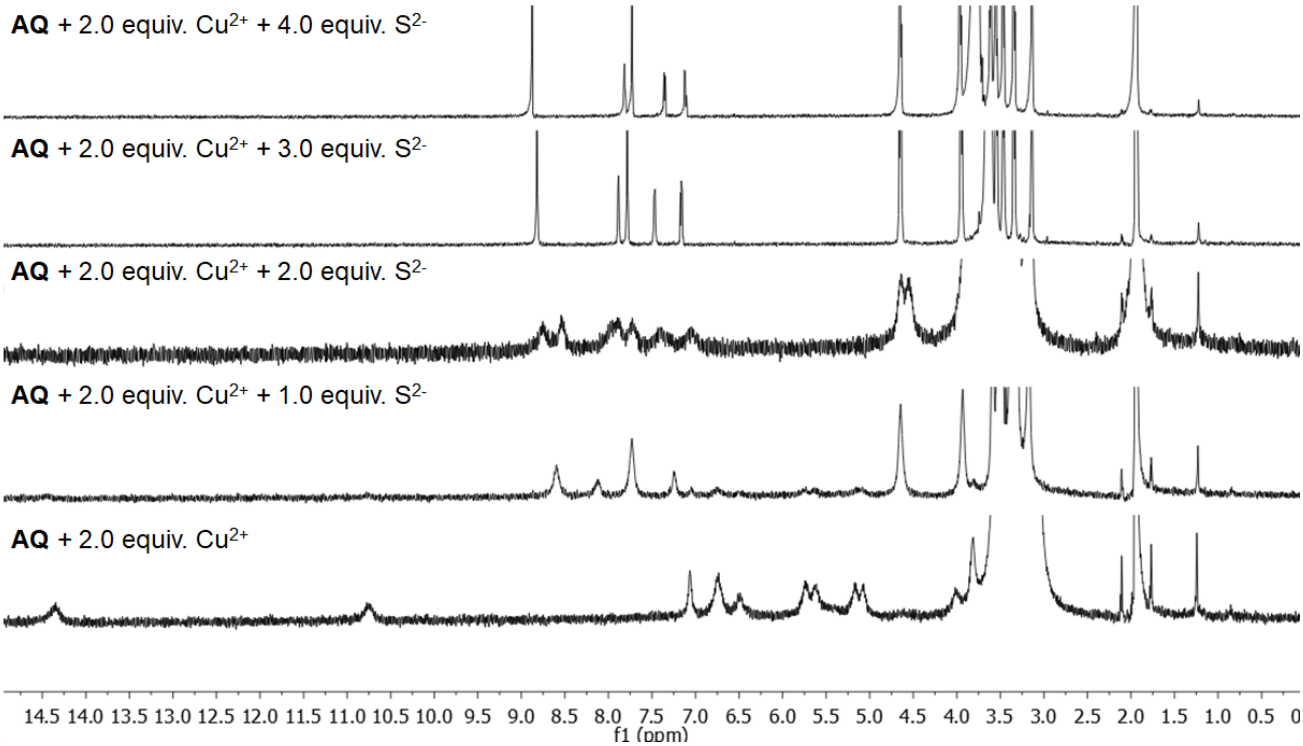

Figure S13. Stacked ^{1}H NMR spectra (400 MHz, CD3CN, 298 K) of **AQ**-Cu^{2+} (5 mM) upon titration with different amount of S^{2-}.

Confocal Imaging

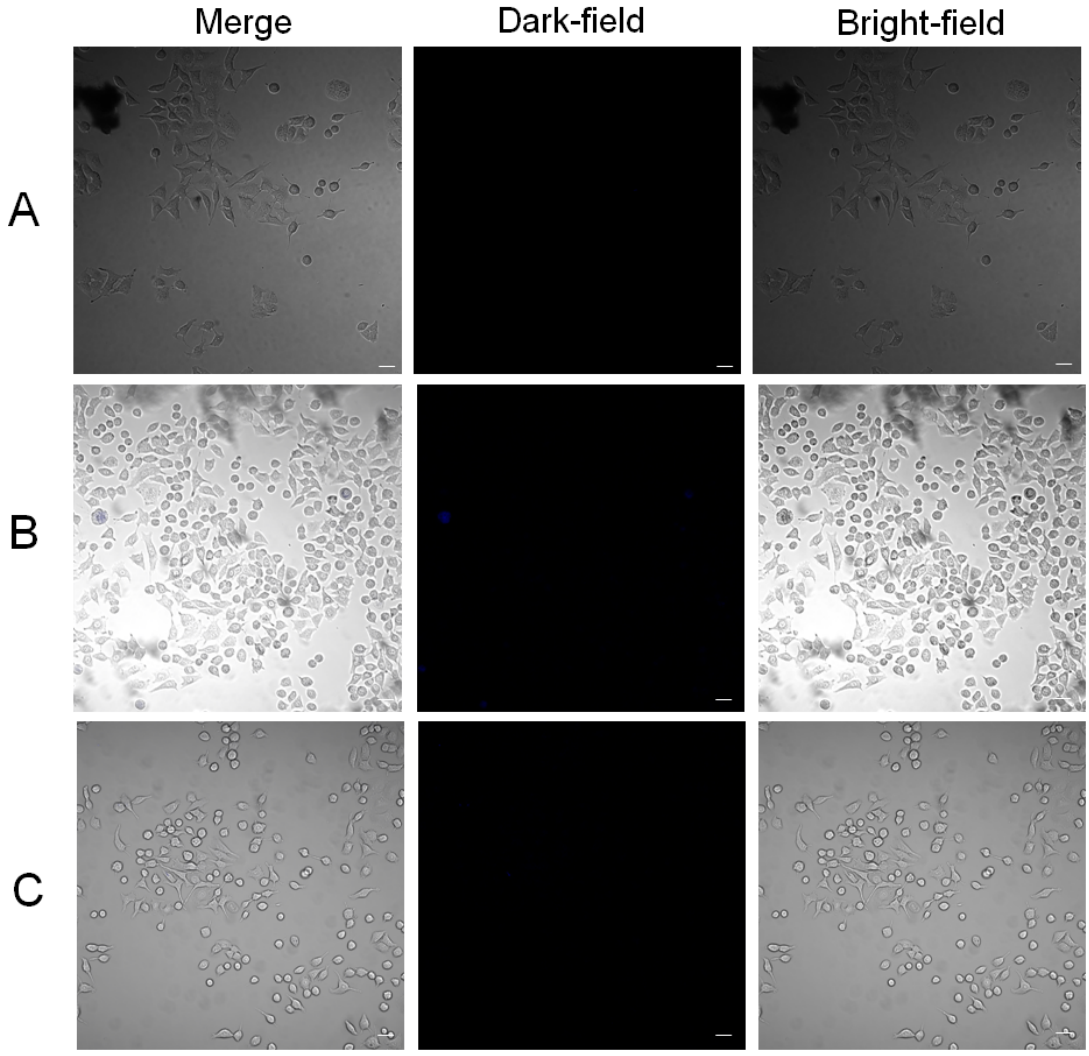

Figure S14. Confocal fluorescence images of A549 cells after the incubation without **AQ**, A) 24 h, B) 10 μM Cu^{2+} for 2 h, C) 10 μM Cu^{2+} for 2 h and 100 μM S^{2-} for another 2 h. Fluorescence transmission images with bright-field, dark-field and merge; scale bar: 25 μm.

NMR Spectra

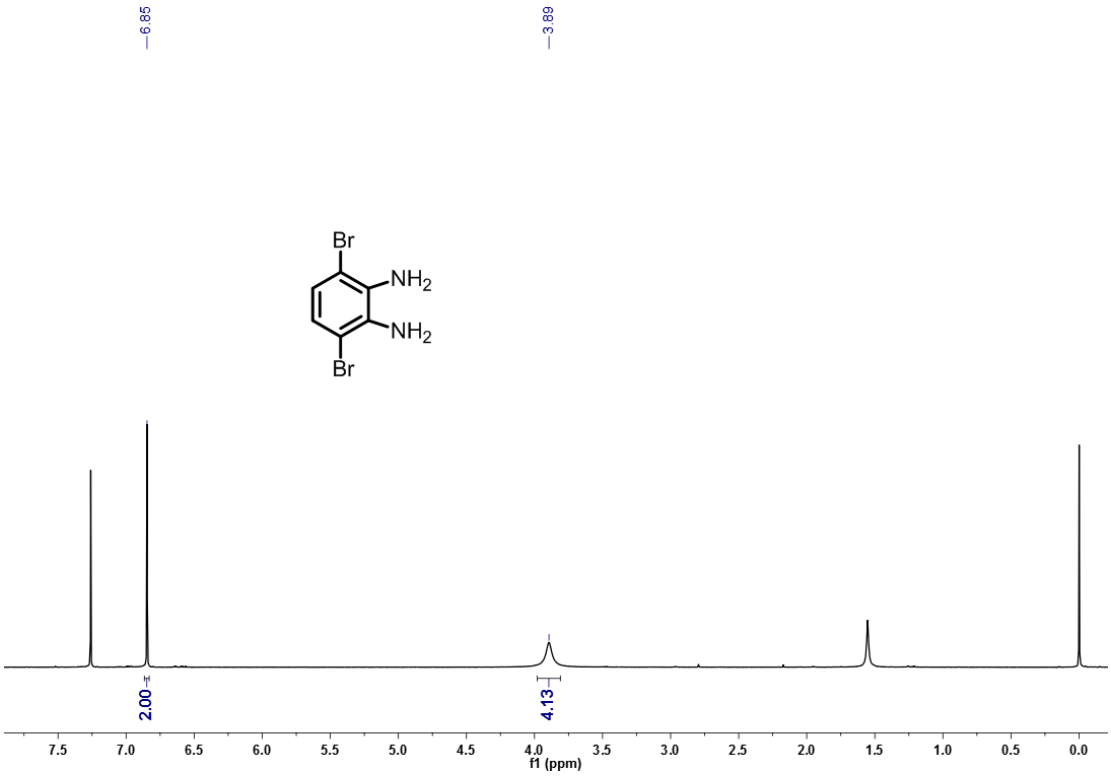

Figure S15. ^{1}H NMR spectrum (400 MHz, $CDCl_3$) of **S1**.

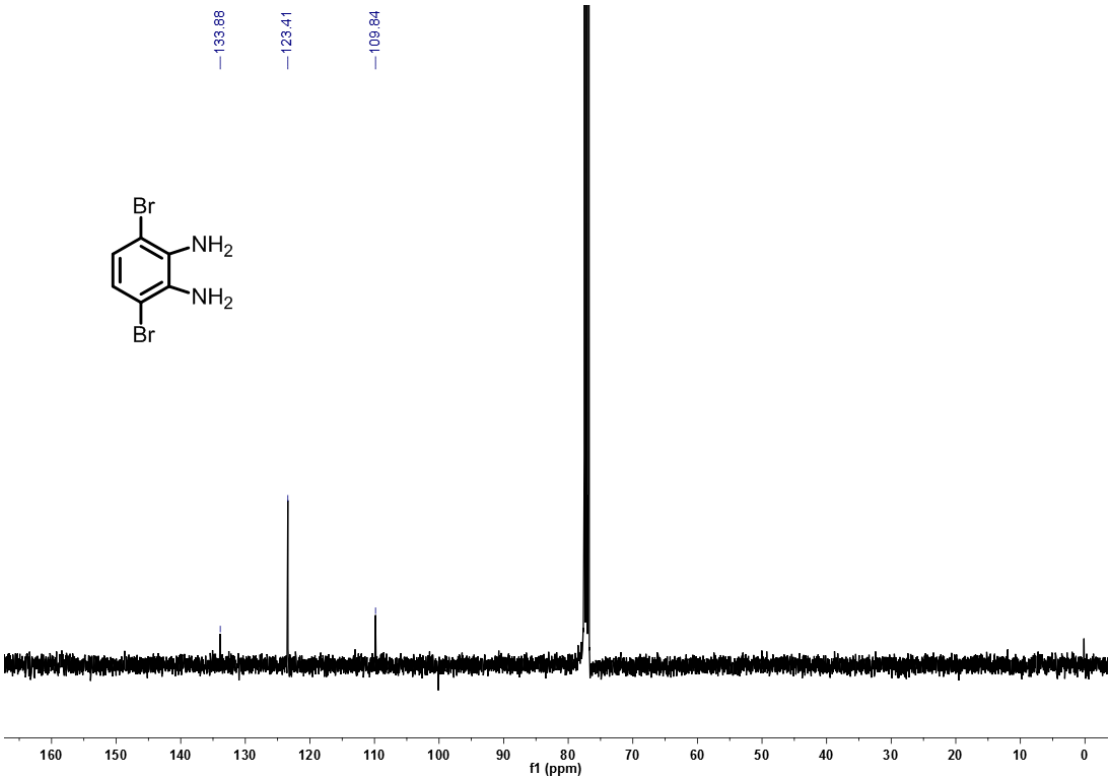

Figure S16. ^{13}C NMR spectrum (101 MHz, $CDCl_3$) of **S1**.

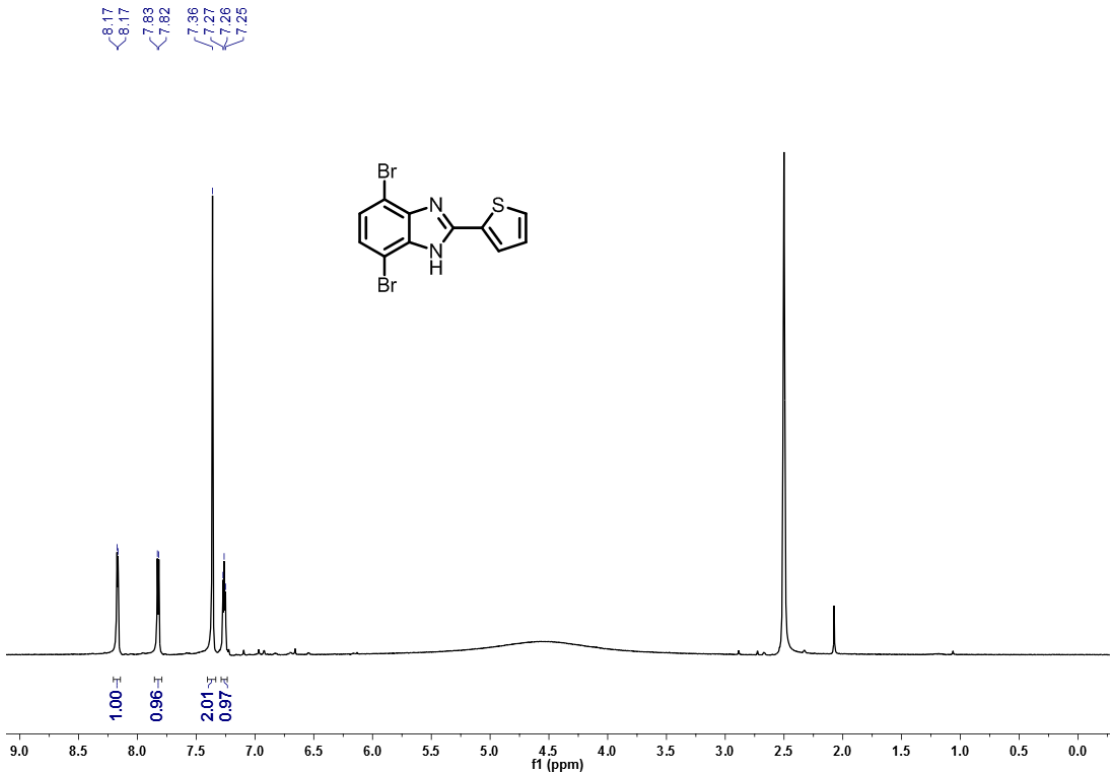

Figure S17. ^{1}H NMR spectrum (400 MHz, d_6-DMSO) of **S2**.

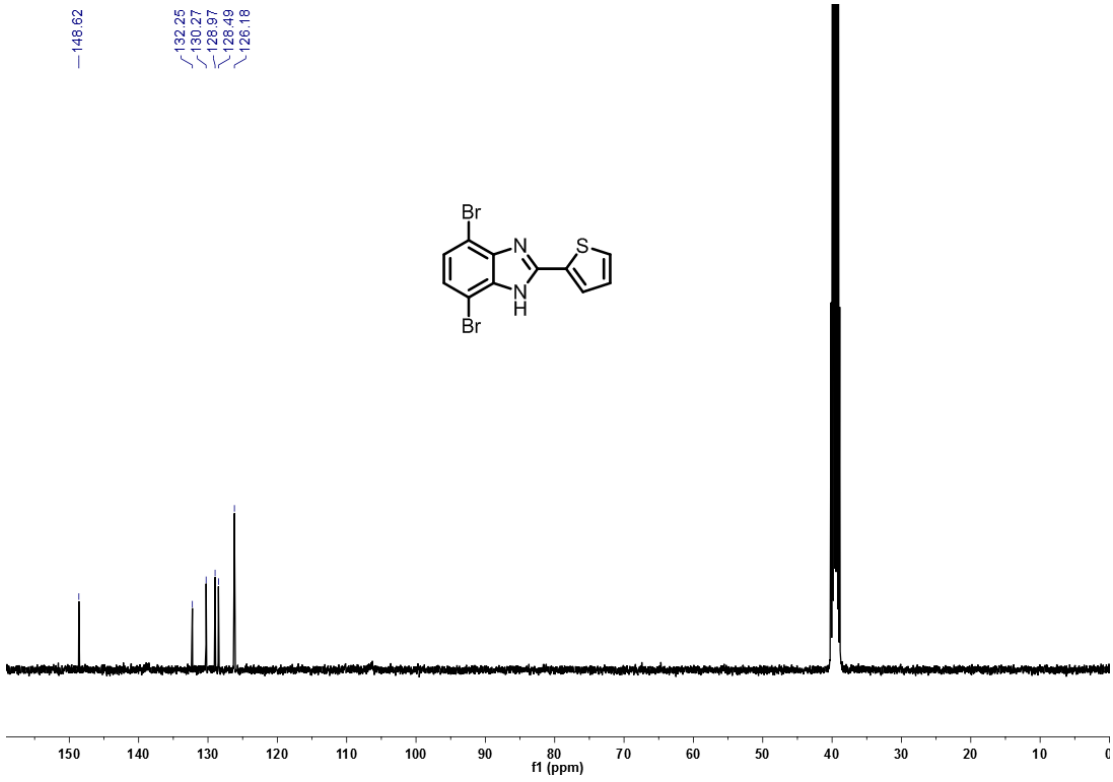

Figure S18. ^{13}C NMR spectrum (101 MHz, d_6-DMSO) of **S2**.

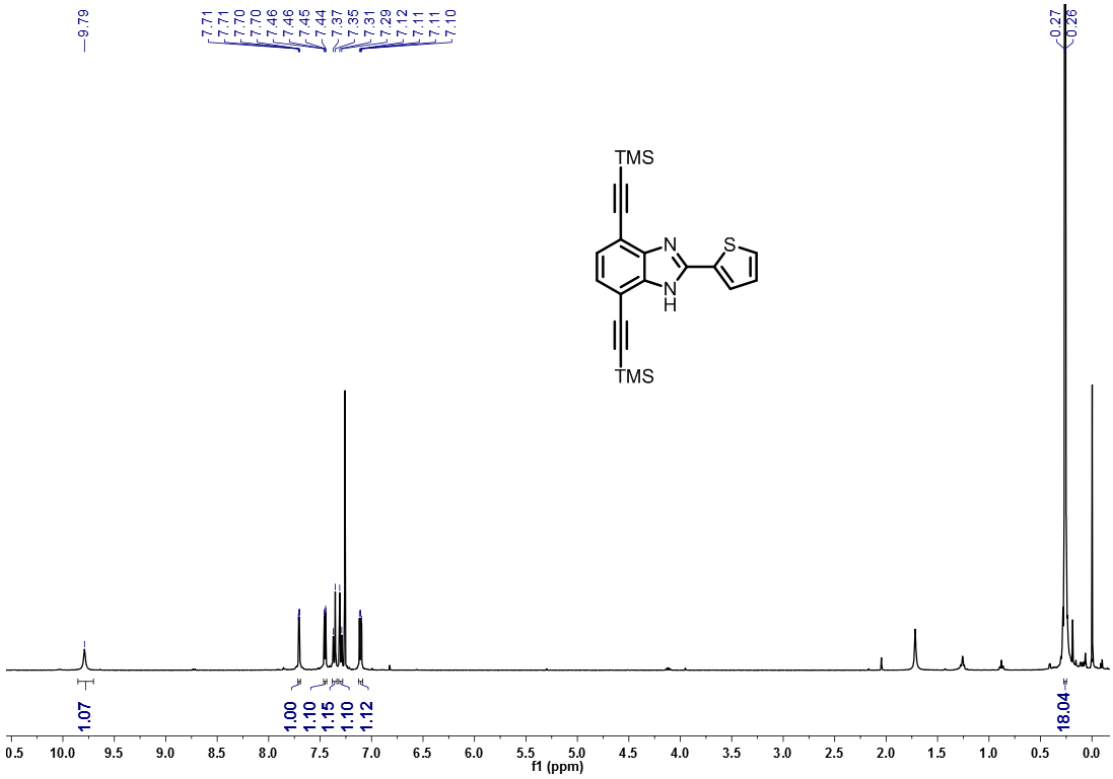

Figure S19. ^{1}H NMR spectrum (400 MHz, $CDCl_3$) of **S3**.

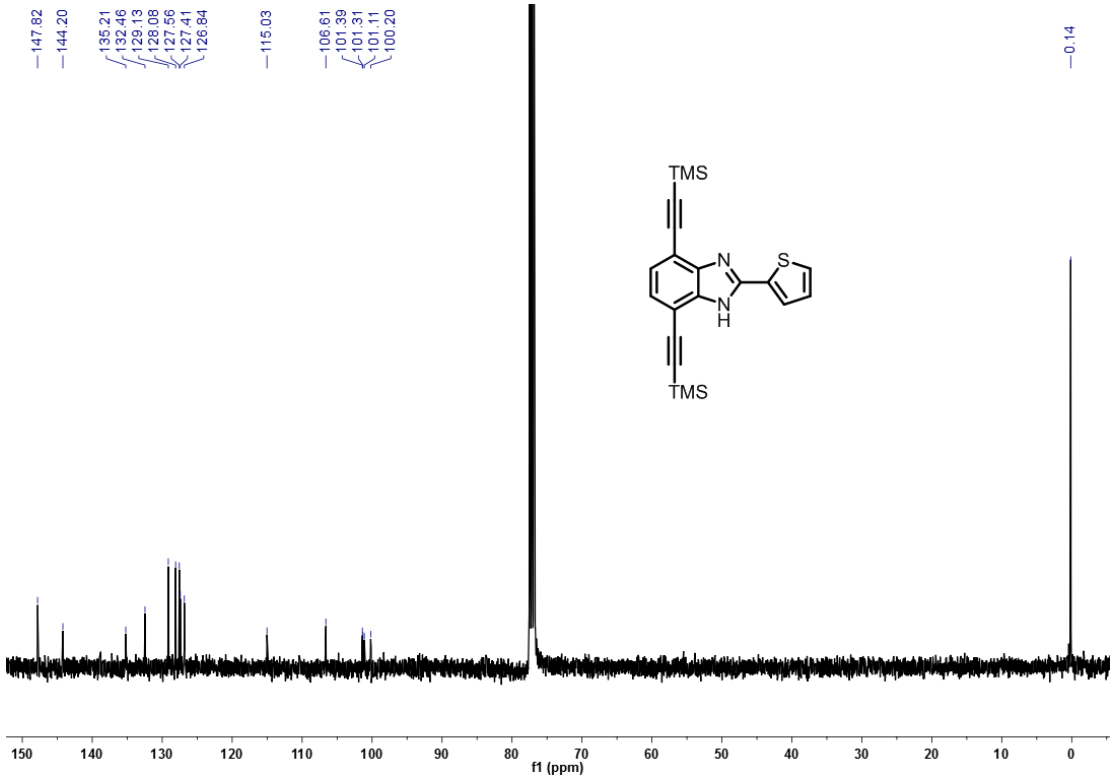

Figure S20. ^{13}C NMR spectrum (101 MHz, $CDCl_3$) of **S3**.

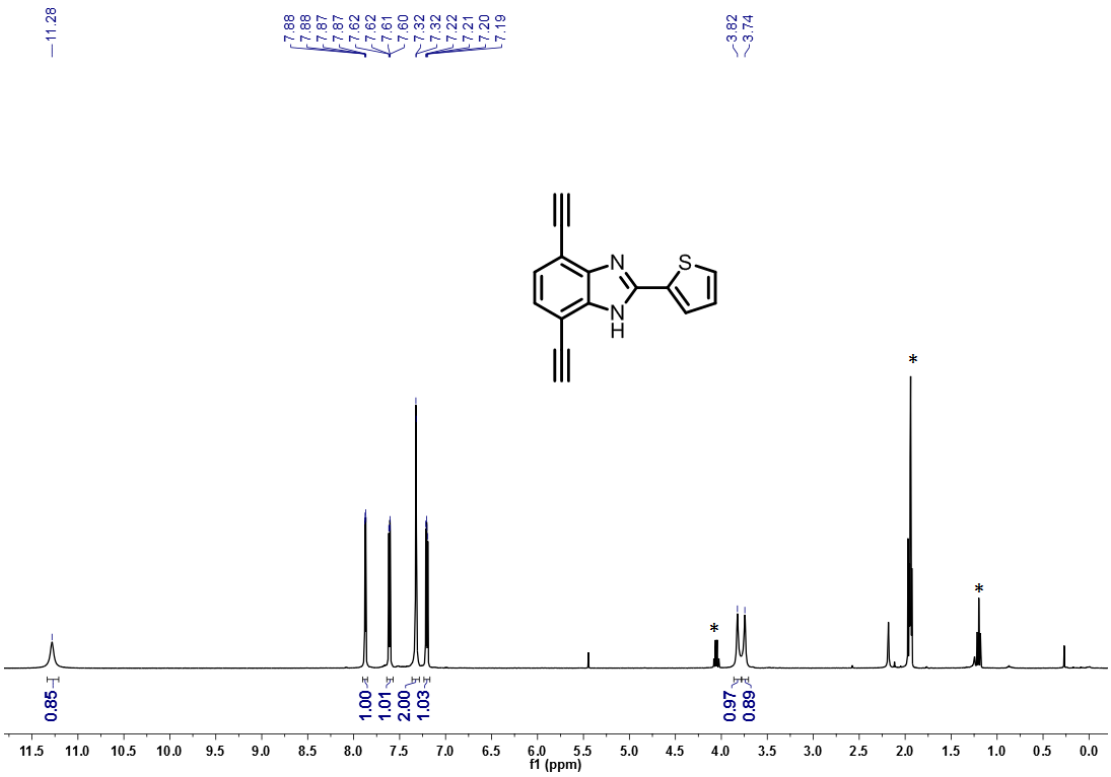

Figure S21. ^{1}H NMR spectrum (400 MHz, CD_3CN) of **S4** (Asterisk: solvent residual signal).

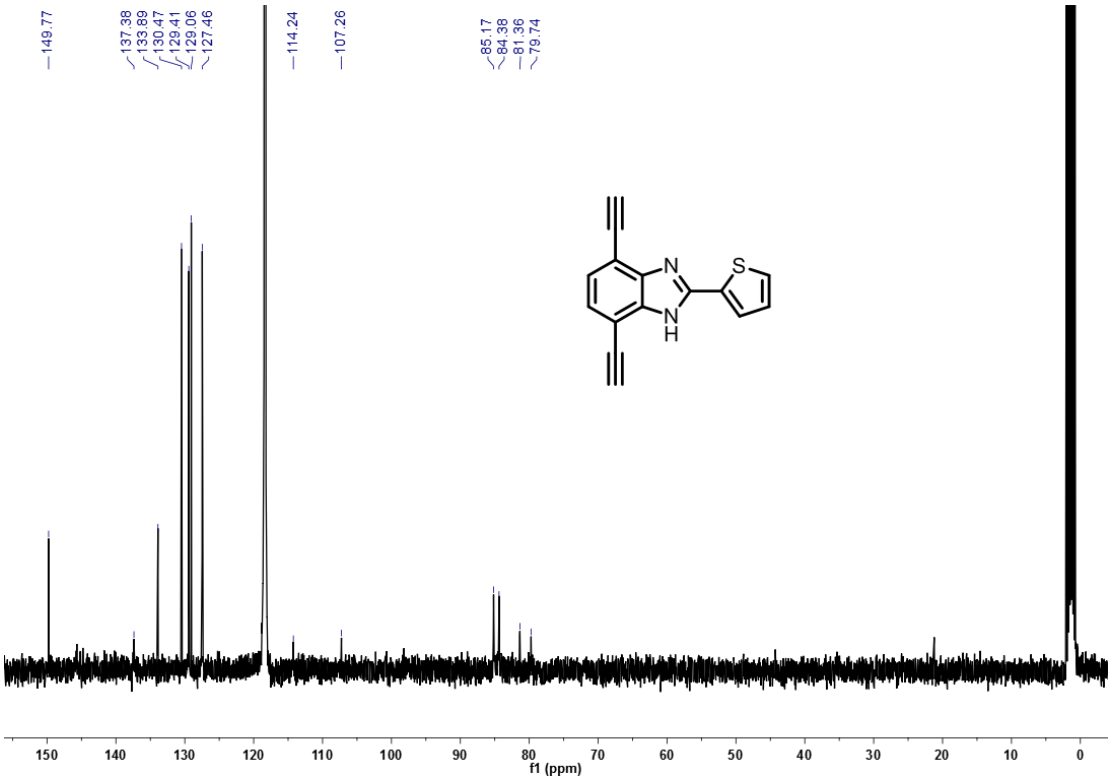

Figure S22. ^{13}C NMR spectrum (101 MHz, CD_3CN) of **S4**.

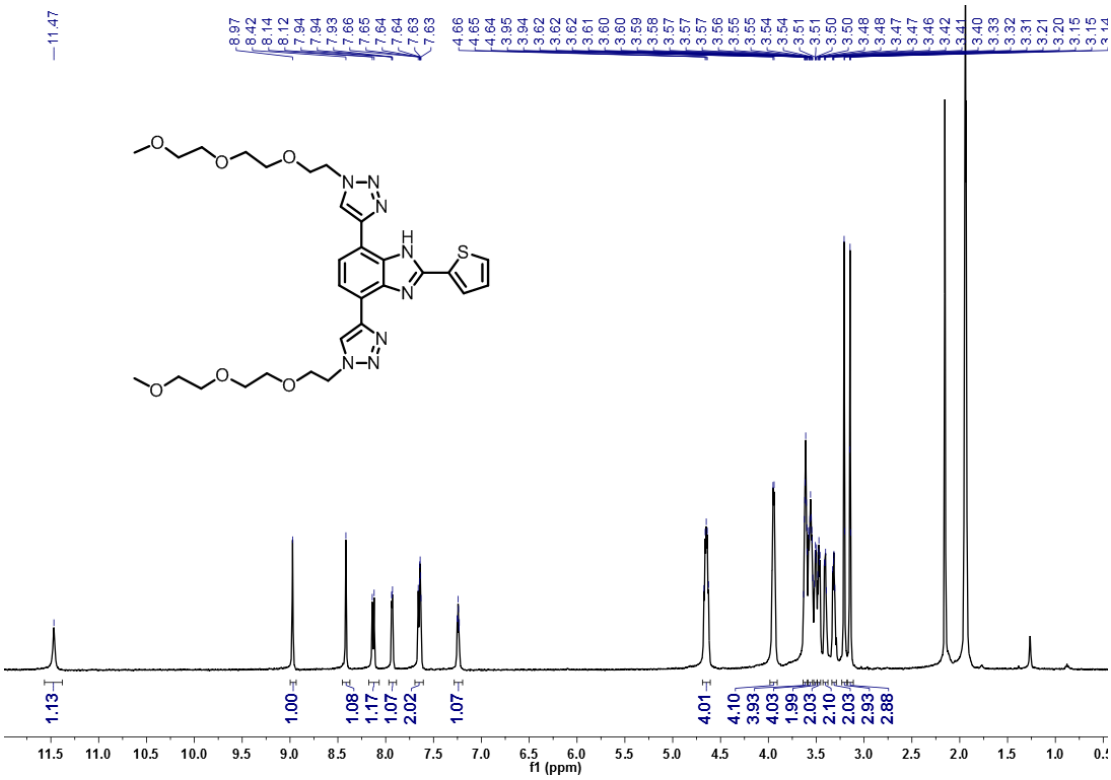

Figure S23. ^{1}H NMR spectrum (400 MHz, CD_3CN) of **AQ**.

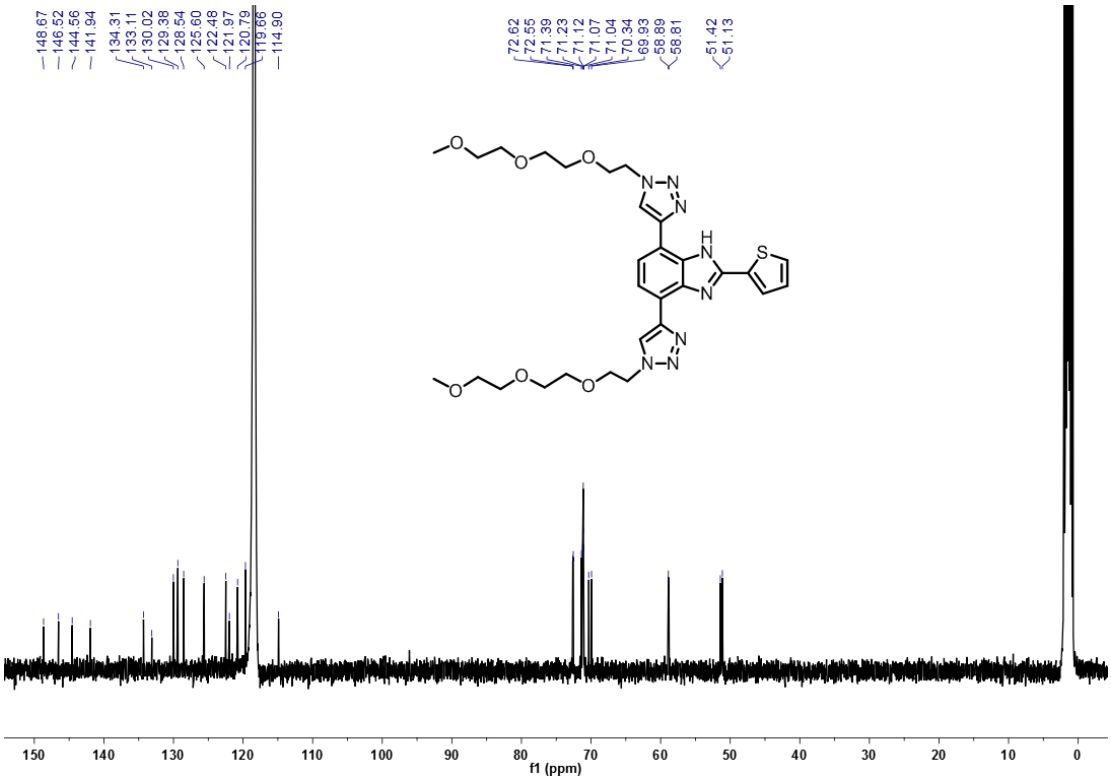

Figure S24. ^{13}C NMR spectrum (101 MHz, CD_3CN) of **AQ**.

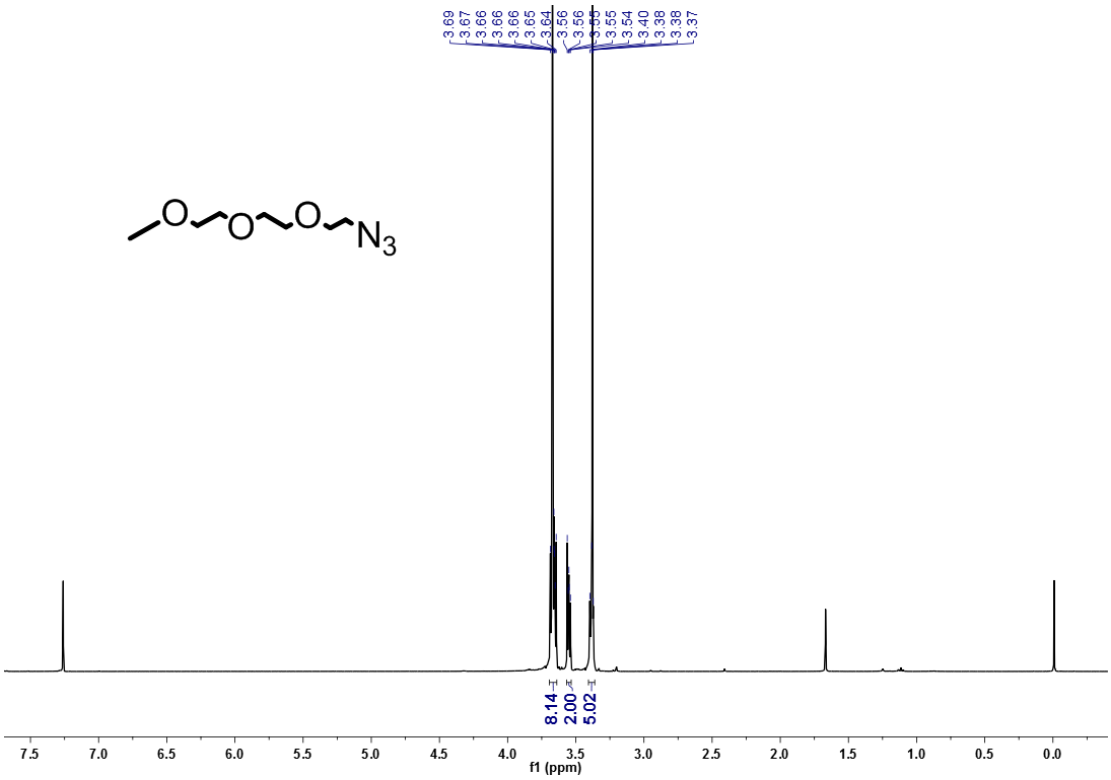

Figure S25. ^{1}H NMR spectrum (400 MHz, $CDCl_3$) of **glycol azide**.

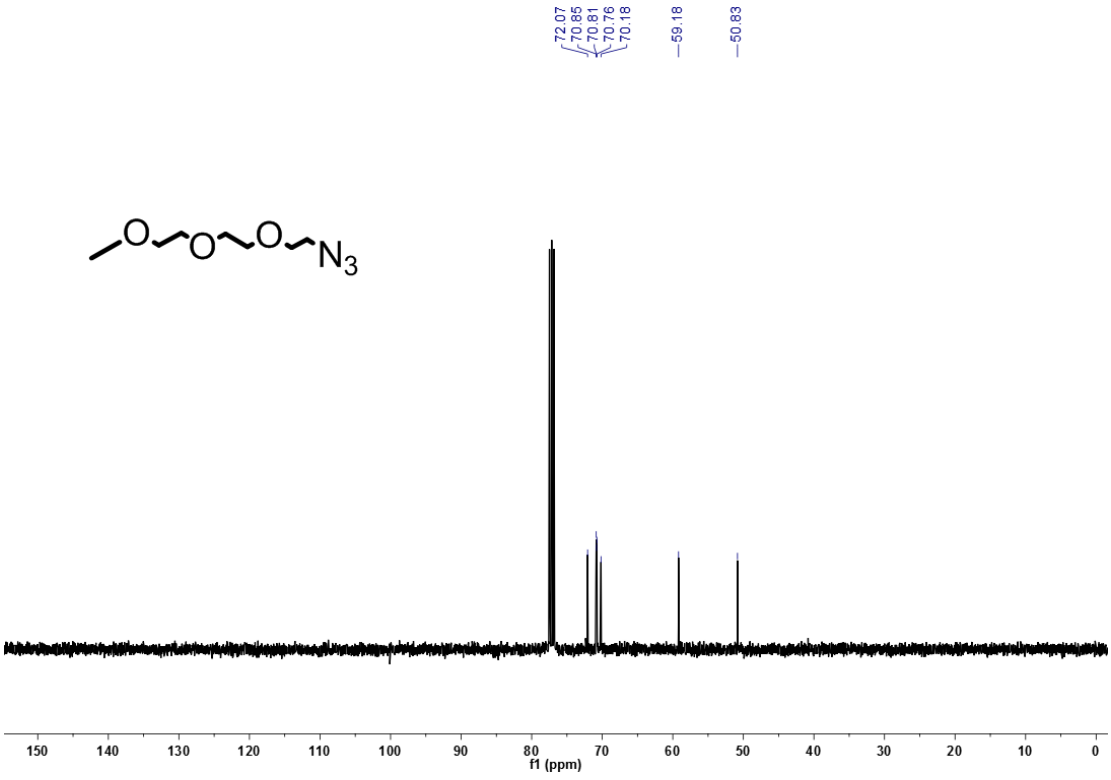

Figure S26. ^{13}C NMR spectrum (101 MHz, $CDCl_3$) of **glycol azide**.

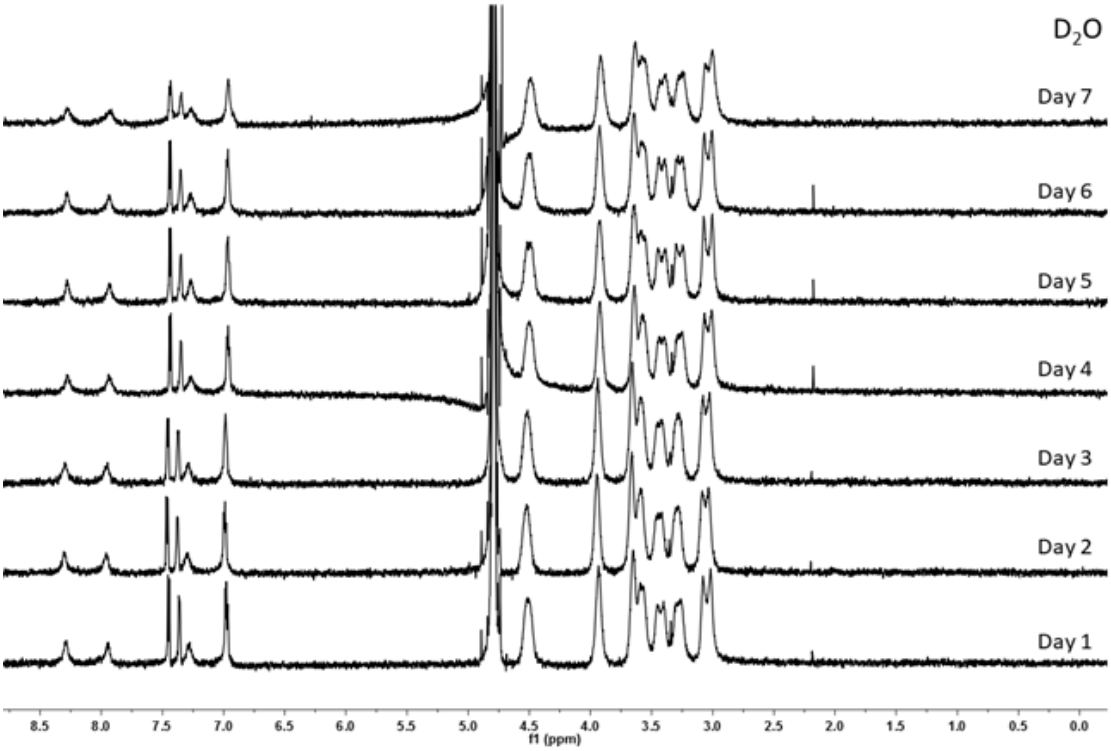

Figure S27. Stacked ^{1}H NMR spectra (400 MHz, D_2O, 298 K) of **AQ** (5 μM) after 7 days in D_2O.

Mass Spectra

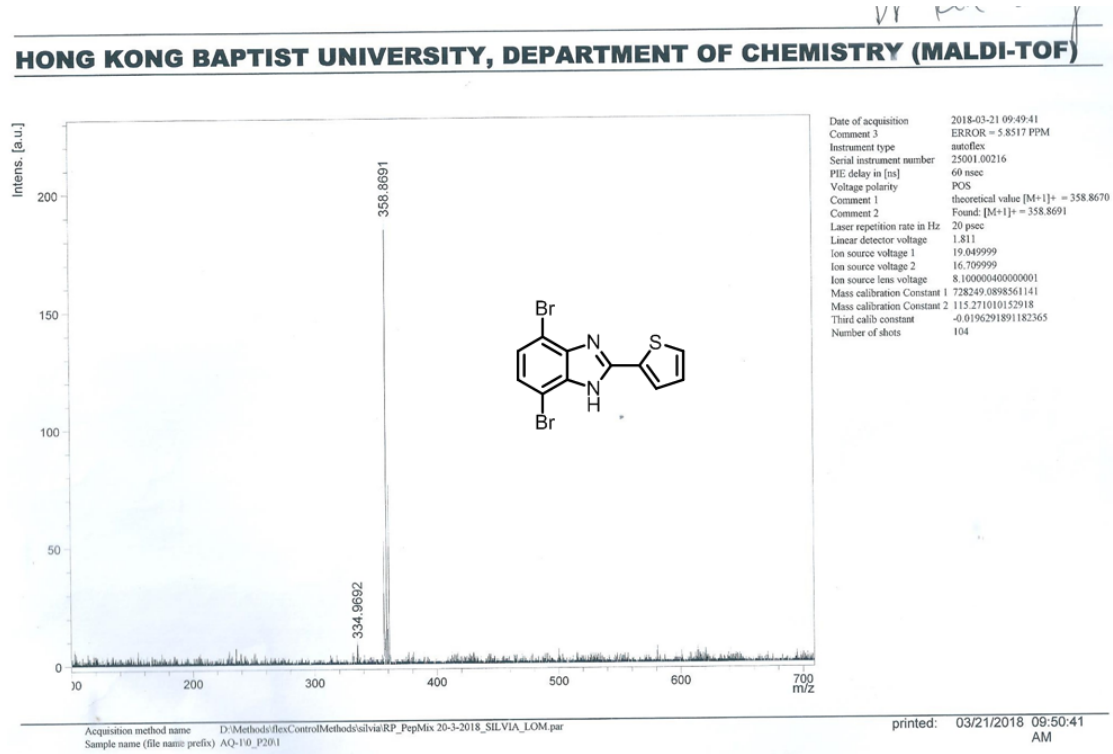

Figure S28. HRMS MALDI-TOF of **S2**.

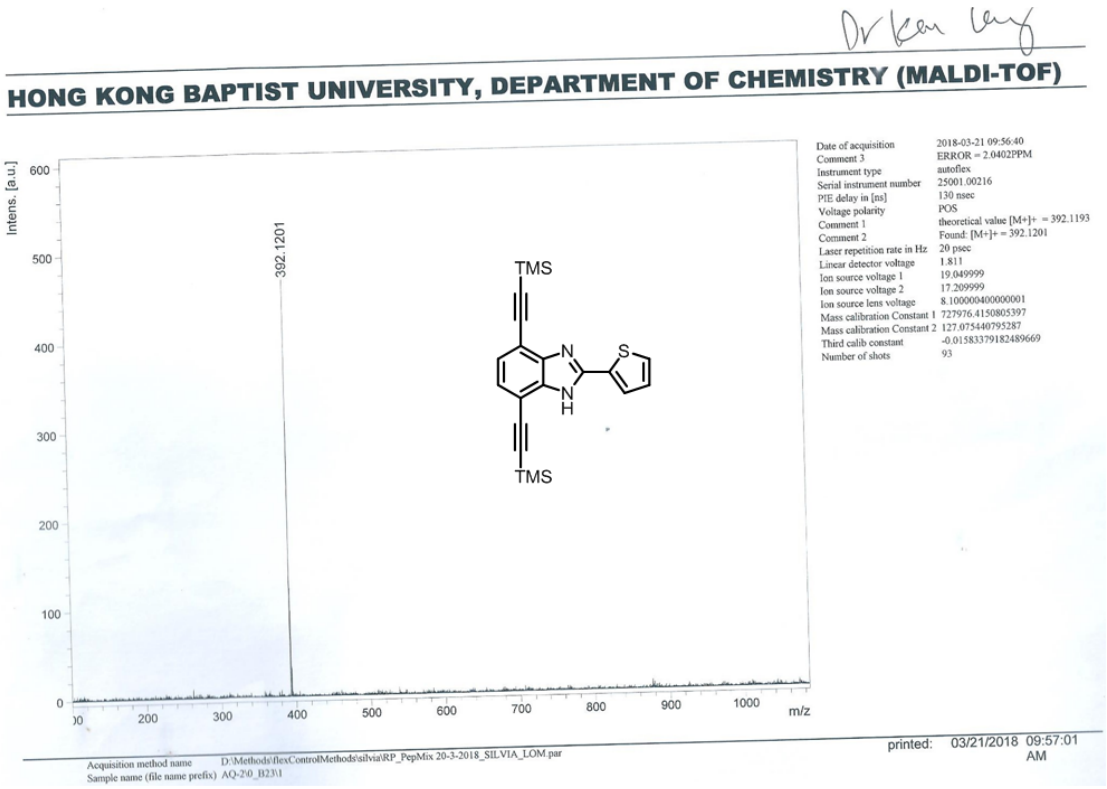

Figure S29. HRMS MALDI-TOF of **S3**.

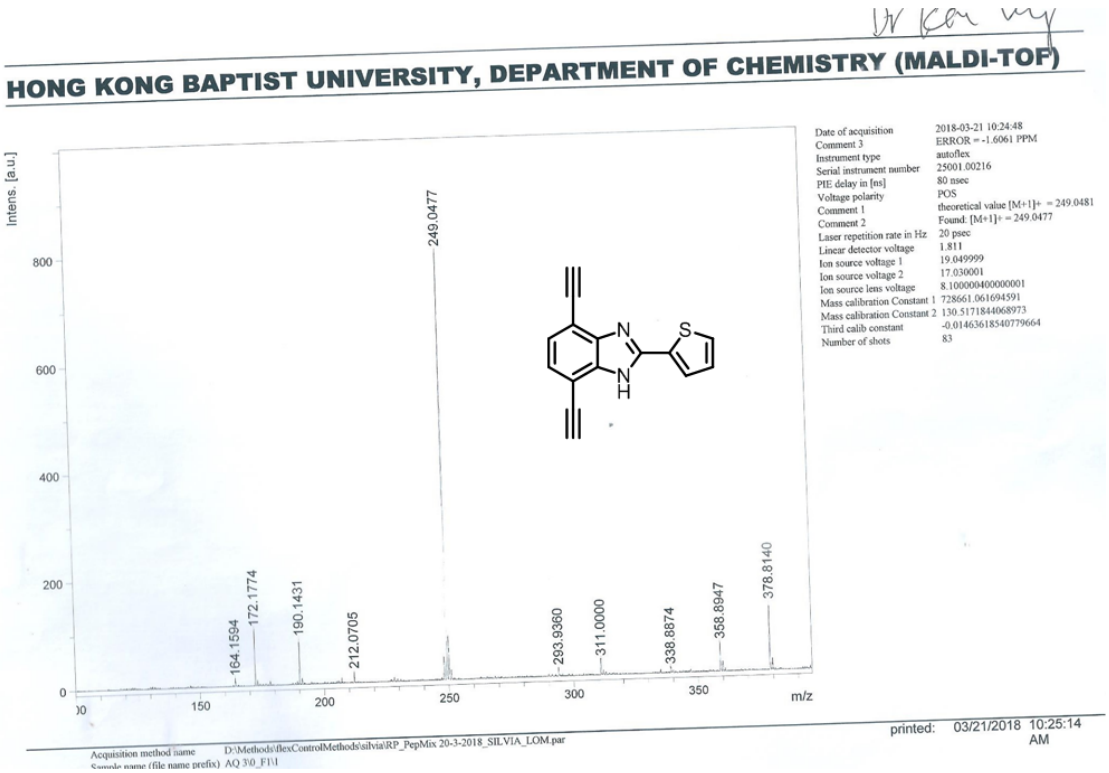

Figure S30. HRMS MALDI-TOF of **S4**.

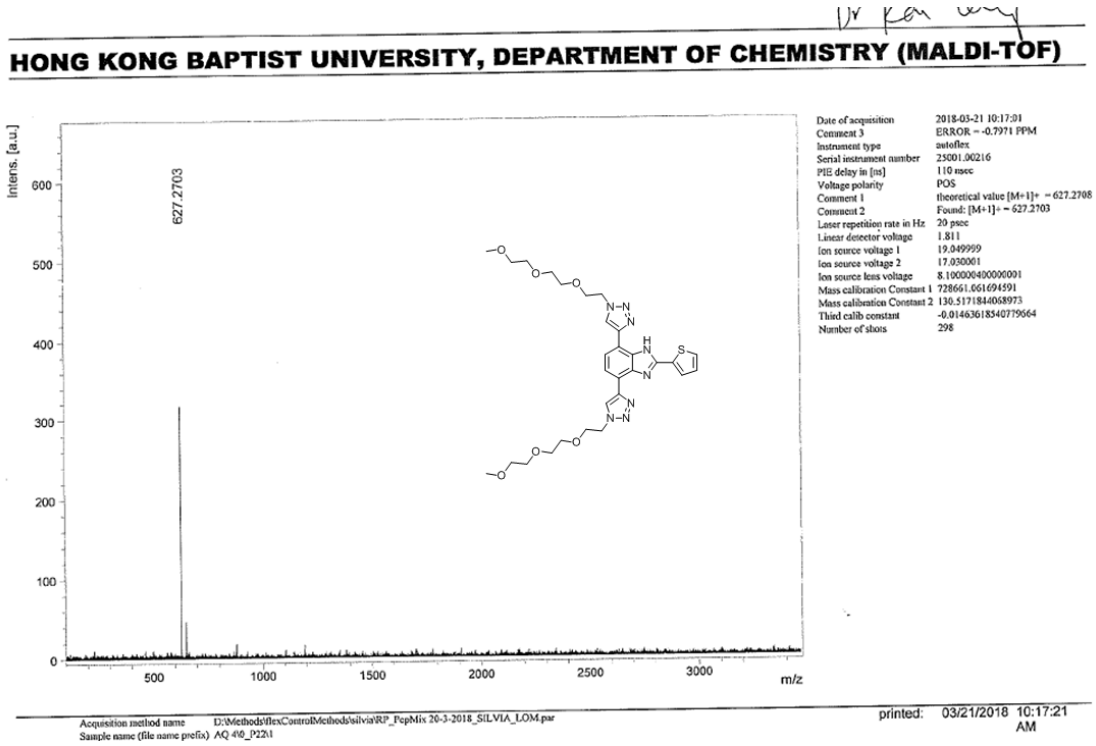

Figure S31. HRMS MALDI-TOF of **AQ**.

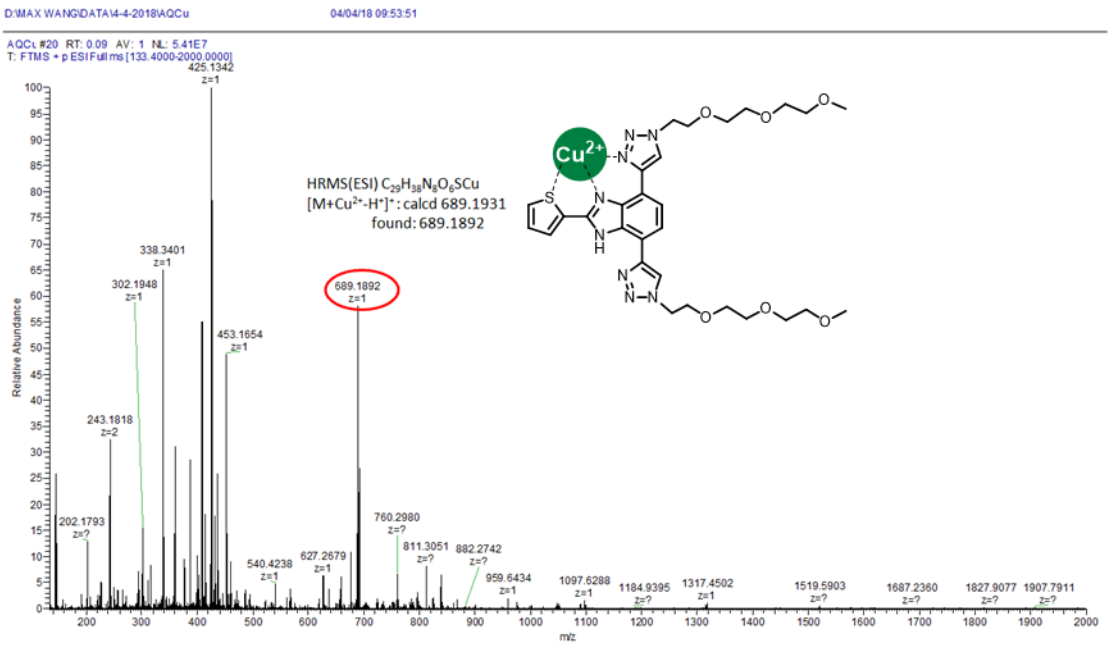

Figure S32. HRMS MALDI-ESI of **AQ**-Cu^{2+}.

References

S1 Yue, X.-L.; Li, C.-R.; Yang, Z.-Y. *Photochem. Photobiol. A Chem.* **2018**, *351*, 1–7.